Study of orientation in polystyrene/poly(vinyl methyl ether) relative to the temperature of phase separation

Essaid Abtal and Robert E. Prud'homme*

Centre de recherche en sciences et ingénierie des macromolécules, Chemistry Department, Laval University, Québec (Qué), Canada G1K 7P4

(Received 25 October 1992; revised 23 February 1993)

Molecular orientation and mechanical properties of polystyrene/poly(vinyl methyl ether) (PS/PVME) miscible blends have been investigated in a broad range of compositions, taking as a reference the temperature of phase separation. Fourier transform infra-red spectroscopy and birefringence have been coupled to characterize the state of orientation of each component of the blend. It is found that the orientation decreases progressively with an increase in the amount of PVME in the blend, and that a close relation holds between the Young's modulus and the overall orientation. The results are interpreted in terms of free-volume variations with the distance to the glass transition temperature. At the initial stage of deformation, the relation between modulus and orientation is analysed using the rubber elasticity theory, whereas at larger deformations, the strain–orientation relation is properly modelled using a constitutive equation derived from the Doi–Edwards molecular theory.

(Keywords: blends; orientation; mechanical properties)

INTRODUCTION

Deformation mechanisms in polymer blends are, in general, complex in comparison to those of homopolymers. Experiments that measure the molecular orientation of each component, during the deformation, allow the analysis of these mechanisms at the molecular level. Such investigations are of particular interest in understanding the relations between orientation and physical properties, and also in developing phenomenological models describing the deformation and the viscoelastic behaviour of this class of materials.

In that context, many studies of the orientation in polymer blends have been reported. For example, the early work of Hubbell and Cooper[1,2] on miscible and immiscible poly(caprolactone)-based polymer mixtures and the comprehensive studies of Jasse, Monnerie and co-workers[3–5] on various miscible blends led to the conclusion that, even with miscible blends, the two polymers orient differently when the glass transition temperature (T_g) is taken as the reference temperature. However, it is clear from these studies that the mechanisms of orientation in polymer blends are still not completely understood.

In the present study, we have selected, for orientation measurements, the polystyrene/poly(vinyl methyl ether) (PS/PVME) system which represents, in our opinion, an excellent model. On the one hand, it is completely amorphous, hence no complication due to the presence of a crystalline phase is expected. On the other hand, this blend, which is miscible at the molecular level[6,7], exhibits a lower critical solution temperature which allows the possibility of comparing the orientation behaviour in the miscible and heterogeneous states. Indeed, the phase diagram of the PS/PVME binary mixture, determined from cloud-point measurements as described in the Experimental section, exhibits three regions of interest in which the viscoelastic and mechanical behaviour may be, a priori, quite different (*Figure 1*). The mechanisms of chain relaxation are not the same if the system is above or below its T_g, and furthermore, in the phase-separated state, the mechanical response to a step deformation may depend upon additional parameters such as size, nature and morphology of the phase domains. Our initial investigation focuses on the region between T_g and the temperature of phase separation (T_c). In this zone, the blend is miscible and two temperatures of reference can be easily defined.

1. T_g can be considered as a reference for chain mobility, since the relaxation motions become faster when increasing the distance from T_g. However, a recent study[8] on poly(methyl methacrylate) (PMMA) has shown that this is not an ideal reference state since two samples of PMMA, differing only by their degree of tacticity, exhibit different orientation behaviour even when the distance to T_g is kept constant.
2. T_c has been taken, in the first approximation, as a reference to characterize the state of specific interactions which are responsible for the miscibility between PS and PVME. The closer the temperature to T_c, the weaker the interaction between the dissimilar chains. In the limiting case, i.e. at T_c, phase separation is induced.

The main objective of this work is to analyse the orientation behaviour of PS/PVME blends, coupling

* To whom correspondence should be addressed

0032-3861/93/224661-08

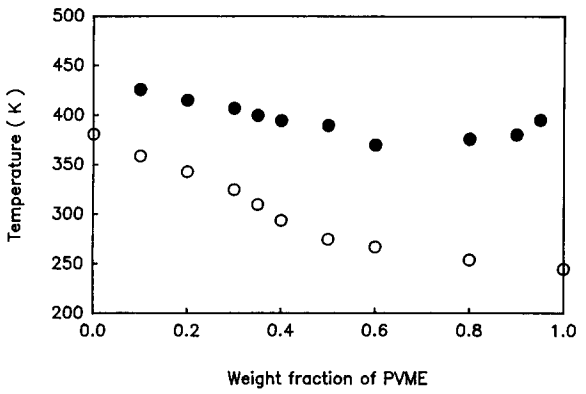

Figure 1 Phase diagram of the PS/PVME blend: ●, T_c; ○, T_g

*FT*i.r. spectroscopy and birefringence, at $T_c - 62$, i.e. when the difference between the stretching temperature and the temperature of demixing is kept constant. At that reference temperature, the data of Han *et al.*[9,10] show that the X_{12} thermodynamic interaction parameter changes monotonically and very slightly with blend composition. For instance, $(X_{12}/v_0) \times 10^4$ ranges between -2.3 and -3.4 when the weight fraction, w_2, of PVME varies from 0.1 to 0.8 (v_0 is the molar volume of a reference cell). In comparison, at $T_g + 10$, $(X_{12}/v_0) \times 10^4$ ranges from -2.2 at $w_2 = 0.1$, to -5.6 at $w_2 = 0.5$. In other words, by taking $T_c - 62$ as the stretching temperature, the strength of specific interactions between PS and PVME is kept roughly constant and the variations observed in orientation must be attributed to other factors.

THEORY

In the case of a uniaxial mode of deformation, the orientation of a structural unit of a polymer chain can be described by an orientation function $f(\theta)$, where θ is the angle between the structural unit axis and the stretching direction[11]. It is assumed that the distribution of the structural units is random in the plane perpendicular to the stretch direction. The orientation function can be developed as a series of Legendre polynomials in $\cos\theta$:

$$f(\theta) = \sum_{n=0}^{\infty} (n+\tfrac{1}{2}) \langle P_n(\cos\theta) \rangle P_n(\cos\theta) \quad (1)$$

where

$$\langle P_n(\cos\theta) \rangle = \int_0^{\pi} f(\theta) P_n(\cos\theta) \sin\theta \, d\theta \quad (2)$$

To evaluate precisely $f(\theta)$, the different moments $\langle P_n(\cos\theta) \rangle$ of the orientation function must be determined. However, for a simple deformation process, the second moment $\langle P_2(\cos\theta) \rangle$ is adequate to describe properly the state of orientation[12].

Different techniques have been used to measure $\langle P_2(\cos\theta) \rangle$. Among them, birefringence and i.r. dichroism are usually used as complementary methods to analyse the molecular orientation of multicomponent blends. In the case of an amorphous homopolymer, the birefringence Δ is directly related to $\langle P_2(\cos\theta) \rangle$ by[11,13]:

$$\Delta = \Delta o \langle P_2(\cos\theta) \rangle \quad (3)$$

where Δo is the intrinsic birefringence of the material. For a binary mixture, the measured birefringence can be written:

$$\Delta = \phi_1 \Delta o_1 \langle P_2(\cos\theta_1) \rangle + \phi_2 \Delta o_2 \langle P_2(\cos\theta_2) \rangle + \Delta f \quad (4)$$

where $\langle P_2(\cos\theta_2) \rangle$, Δo_i and ϕ_i are the second moment of the orientation function, the intrinsic birefringence and the volume fraction of the ith component, respectively. Δf is the form birefringence related to the difference of refractive index between the two polymers. However, in the case of miscible blends, this term is neglected[14,15].

The second moment of the orientation function can also be calculated from *FT*i.r. measurements. The dichroic ratio D of any i.r. absorption band is related to $\langle P_2(\cos\theta) \rangle$ by[11]:

$$\langle P_2(\cos\theta) \rangle = (D-1)(D_0+2)/(D+2)(D_0-1) \quad (5)$$

where $D = A_{\parallel}/A_{\perp}$, which is the ratio of the absorbance for the electric vector of the incident radiation polarized parallel and perpendicular to the stretching direction, respectively. $D_0 = 2\cot^2\alpha$, α being the angle between the transition moment vector of the vibration under consideration and the local chain axis. For polymer blends, the orientation of each component can be determined provided that specific bands, corresponding to vibration modes with well-defined transition moment vectors, are observed for the two polymers. This is not the case for the PS/PVME system. However, the coupling of *FT*i.r. and birefringence measurements allows the characterization of the individual orientation of the two chains, as will be explained later.

EXPERIMENTAL

Materials

Atactic PS and PVME were used in this study. PS had $M_w = 300\,000$ and a polydispersity index of 1.06. PVME had $M_w = 44\,000$ and a polydispersity of 2.3. These values were determined by size exclusion chromatography in tetrahydrofuran at 298 K using PS standards.

Films of different compositions and thicknesses were cast from benzene solutions onto a glass plate. They were first air-dried for 1 day, and then the last traces of solvent were removed under vacuum at $T_g + 30$ for 36 h.

Birefringence and mechanical property measurements

Birefringence and mechanical property measurements were conducted using an Instron tensile tester, model 1130, with a controlled temperature sample compartment constructed in our laboratory. For the birefringence measurements, an He/Ne laser source was placed at the back of the sample compartment and a Soleil–Babinet compensator at the front. It was therefore possible to measure the birefringence and the stress–strain curves simultaneously, at a fixed temperature. The samples, which had an initial thickness of 200 μm, a width of 3.5 mm and a length of 45 mm, were stretched at a strain rate of 5 cm min^{-1}. The birefringence measurements required a pause time which, however, did not exceed 100 s.

Infra-red dichroism measurements

*FT*i.r. measurements were carried out using a Mattson Sirius 100 spectrophotometer with a rotating wire-grid polarizer (Specac UK). An i.r. cell, constructed in our laboratory and adapted to the sample compartment of

the spectrophotometer, allowed the sample to be heated to a given temperature and to be stretched at a constant strain rate of 5.0 cm min^{-1}. The sample was stretched to the desired draw ratio and the stretching process was then interrupted for about 100 s while the two polarized spectra were recorded. For each polarization, the phase correction was executed separately, and 30 scans were co-added with a maximum optical retardation of 0.52 cm, and triangularly apodized to yield a resolution of 4 cm^{-1}. I.r. dichroism was calculated from the peak height intensity measured in absorbance. All spectral manipulations were executed with software provided by Mattson. The samples had an initial width of 5.0 mm and initial length of 20 mm. The thickness was adjusted between 40 and 100 μm, depending on blend composition, in order to maintain the i.r. absorbance below unity and to avoid deviations from the Beer–Lambert law.

For both birefringence and i.r. experiments, values of the orientation function reported in this paper are averages of at least three measurements on different samples with a reproducibility estimated to be about 10%.

T_g and T_c measurements

To construct the PS/PVME phase diagram, T_g was determined with a Perkin–Elmer DSC-4 differential scanning calorimeter, equipped with a thermal analysis data station and calibrated with indium, at a heating rate of 20 K min^{-1}; T_c was determined using a Zeiss optical microscope, a Zeiss photometer and a Mettler hot stage. The samples were heated from room temperature to the phase-separated state, at a heating rate of 2 K min^{-1}. T_c was then taken as the temperature where the intensity begins to increase (cloud point).

As can be seen in *Figure 1*, a single T_g, intermediate to those of the pure components, is observed at each composition, indicating the miscibility of the system in the entire composition range. On the other hand, the variation of T_c with composition is monotonic and almost linear in a broad range of composition, with a minimum at a PVME weight fraction of about 0.75 and at a temperature of 370 K, in good agreement with the data of Hashimoto *et al.*[16]. Furthermore, the miscibility window, i.e. the interval between T_g and T_c, increases from 60 K at low PVME content to about 120 K at high PVME concentration.

RESULTS

Overall orientation and modulus

The overall orientation of the samples was characterized by birefringence measurements. *Figure 2* gives the increase of the birefringence as a function of the draw ratio λ, at $T_c - 62$, for different blend compositions. It is observed that the data points vary almost linearly with λ. The continuous lines are the result of a simulation of the data on the basis of the Doi–Edwards theory, as will be explained later. This orientation behaviour can also be described by plotting the initial slope, $-d\Delta/d\lambda$, of the curves of *Figure 2* as a function of the PVME percentage (*Figure 3*). It is seen that the overall orientation decreases with an increasing amount of PVME in the blend. Young's moduli (E), for different compositions of the blend, were calculated from the initial slopes of the stress–strain curves. These values, when plotted as a function of the PVME blend concentration, exhibit the same variation as the overall orientation (*Figure 3*). This similar behaviour leads to a linear relation between $-d\Delta/d\lambda$ and E, as illustrated in *Figure 4*.

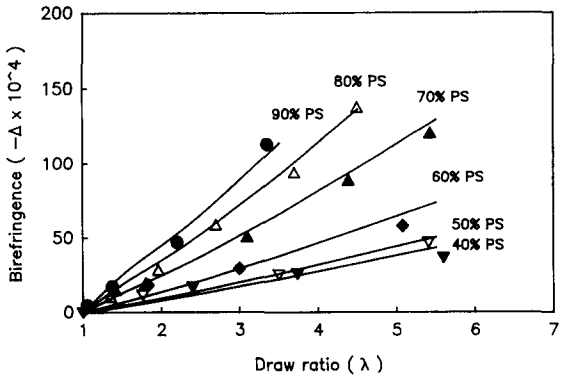

Figure 2 Birefringence, Δ, as a function of the draw ratio, λ, for different blend compositions at a stretching rate of 5 cm min^{-1}. Continuous lines are drawn using equation (32)

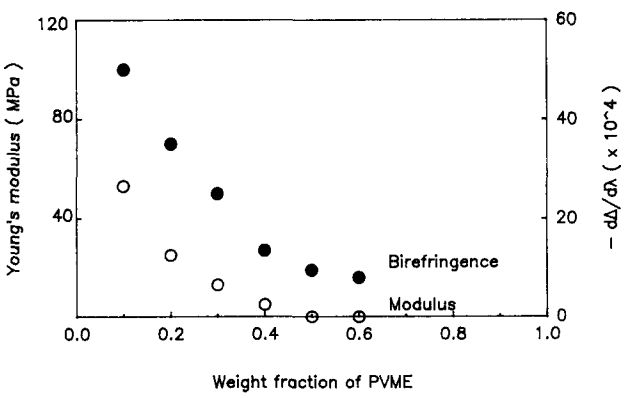

Figure 3 Initial slope of $\Delta = f(\lambda)$ and Young's modulus, E, as a function of the weight fraction of PVME

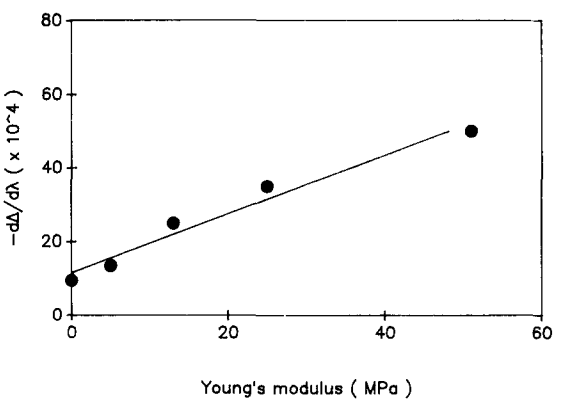

Figure 4 Initial slope of $\Delta = f(\lambda)$ as a function of Young's modulus, E, for different blend compositions

PS orientation

The decrease observed in birefringence and Young's modulus as a function of the PVME content may be, a priori, related to an overall decrease of orientation of the two components, or to a preferential decrease in orientation of one of them. In order to examine this point, *FT*i.r. analysis of the PS orientation in the blend was made using the well-isolated 1028 cm^{-1} band, corresponding to the υ_{18a} vibration of the in-plane stretching mode of the C–H groups of the aromatic cycle.

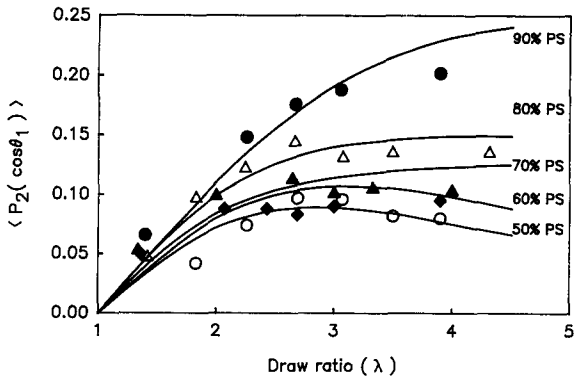

Figure 5 Orientation function $\langle P_2(\cos\theta)\rangle$ of PS as a function of the draw ratio, λ, for different blend compositions at a stretching rate of 5 cm min^{-1}. Continuous lines are drawn using equation (32)

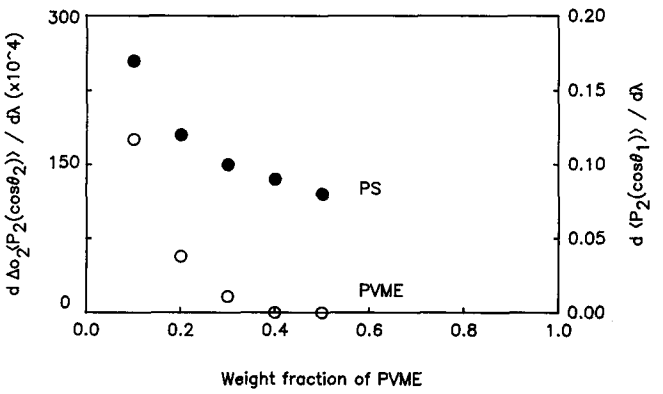

Figure 6 Initial slope of $\langle P_2(\cos\theta)\rangle = f(\lambda)$ and $\Delta o\langle P_2(\cos\theta)\rangle = f(\lambda)$ of PS and PVME, respectively, as a function of the weight fraction of PVME

The vibration is conformationally insensitive, with a transition moment vector perpendicular to the chain axis[17].

Figure 5 shows the variation of $\langle P_2(\cos\theta_1)\rangle$ of PS with the draw ratio, for different compositions. Here also, the solid lines are the result of a simulation using the Doi–Edwards theory. As was observed for the birefringence and Young's modulus, the PS orientation decreases progressively when the fraction of PVME in the blend increases (*Figure 6*).

PVME orientation

The PS/PVME i.r. spectrum exhibits an overlap of a large number of PS and PVME bands[18,19]. For the PVME, only two bands are well isolated. The first one, at 1100 cm^{-1}, is assigned to the asymmetric stretching mode of the C–O–C bond, while the second one, at 2820 cm^{-1}, is assigned to the symmetric stretching mode of the methoxy group[18]. These modes are both related to the side-chain vibrations. Thereafter, an *FT*i.r. determination of the PVME orientation is not possible, since the real conformational structure of the side chain of the PVME in the blend is not known. However, the state of orientation of this polymer may be approximated from the calculation of its dichroic ratio. In the range of composition and temperature studied, D ranges between 1 and 0.98 for the 1100 cm^{-1} band, indicating a weak orientation of PVME in the blend.

The orientation of this polymer can be characterized more accurately by coupling *FT*i.r. and birefringence methods. The contribution $\Delta o_2\langle P_2(\cos\theta_2)\rangle$ of the PVME to the total birefringence is directly related to its state of orientation. According to equation (4), and neglecting the small difference between the density of the two polymers, the volume fractions ϕ_i become weight fractions w_i, and $\Delta o_2\langle P_2(\cos\theta_2)\rangle$ can be expressed as:

$$\Delta o_2\langle P_2(\cos\theta_2)\rangle = (\Delta - w_1\Delta o_1\langle P_2(\cos\theta_1)\rangle)/w_2 \quad (6)$$

To calculate this contribution, we have used the experimental values of Δ and $\langle P_2(\cos\theta_1)\rangle$ reported in *Figures 2* and *5*, whereas Δo_1 was derived from *FT*i.r. and birefringence measurements on pure PS, according to equation (3)[19]. The orientation of PVME exhibits the same trend as that of PS with respect to the blend composition (*Figure 6*). However, it should be noted that the PVME orientation decreases more rapidly than that of PS: above a PVME weight fraction of about 0.3, the PVME chains remain practically unoriented.

ANALYSIS AND DISCUSSION

Models based on the rubber elasticity theory

Due to topological constraints between the chains, amorphous polymers are known to form stable networks if their molecular weight is larger than the critical molecular weight for the formation of stable entanglements (M_c). Consequently, one would expect that, at least at small deformations above T_g, their behaviour could be properly described by the rubber elasticity theory. Making this assumption, an attempt has been made to model the modulus–orientation and strain–orientation relations using the rubber elasticity theory.

Let us begin by looking at the relations between the overall orientation and Young's modulus. For a crosslinked homopolymer, the rubber elasticity theory[20] indicates that the birefringence is proportional to the applied stress. This linear relation has been extended to uncrosslinked amorphous homopolymers by Read[21]. In the case of amorphous miscible blends, one can write:

$$\Delta = w_1C_1\sigma_1 + w_2C_2\sigma_2 \quad (7)$$

where C_i is the stress-optical coefficient and σ_i the applied stress of the ith component. This equation may be rewritten in the form[14]:

$$\Delta = (w_1C_1k_1 + w_2C_2k_2)\sigma = \bar{C}(w_2)\sigma \quad (8)$$

where $k_i = \sigma/\sigma_i$ is the stress-concentrating factor for the ith component and $\bar{C}(w_2)$ the average stress-optical coefficient of the blend. The first derivative of equation (8) with respect to λ leads to:

$$d\Delta/d\lambda = (w_1C_1k_1 + w_2C_2k_2)E = \bar{C}(w_2)E \quad (9)$$

In order to verify the validity of this equation, we have plotted $-(d\Delta/d\lambda)(1/E)$ *versus* w_2. As may be seen from *Figure 7*, a linear relation holds between $\bar{C}(w_2)$ and w_2, in good agreement with the proposed equation. This result illustrates the close relation between the overall orientation and the mechanical properties, and suggests that the blend exhibits a rubber-like behaviour at the initial stage of deformation. This can be understood if one assumes that entanglements, as well as specific interactions between the dissimilar chains, may play, at this stage, the role of actual crosslinks.

Let us pursue the analysis of the relation between strain and orientation. Assuming an affine deformation of the end-to-end vector of the flexible chains, Roe and

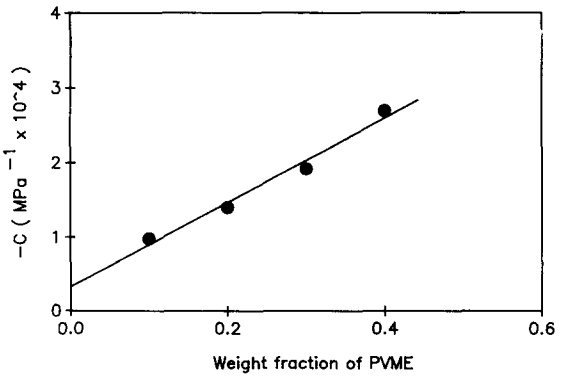

Figure 7 Stress-optical coefficient, C, of the blends as a function of the weight fraction of PVME

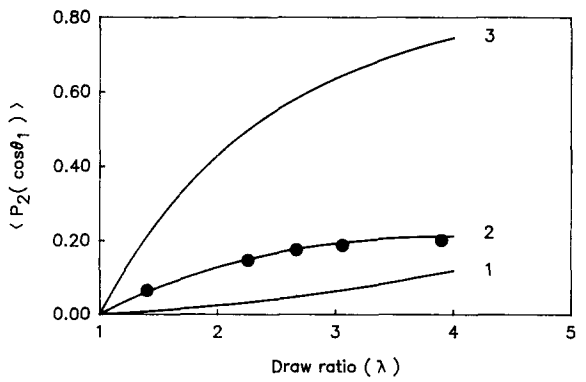

Figure 8 Simulation of the orientation function $\langle P_2(\cos\theta)\rangle$ of PS in the 90% PS blend, by the classic models derived from the rubber elasticity theory. 1, Affine model, $N=29$; 2, model of Raha and Bowden, $N_0=2$, $k=0.5$; 3, pseudo-affine model

Krigbaum[22] developed a rubber-like network theory relating $\langle P_2(\cos\theta)\rangle$ to the strain λ:

$$\langle P_2(\cos\theta)\rangle = (1/5N)(\lambda^2 - 1/\lambda) + (36/875N^2)(\lambda^4 + \lambda/3 - 4/3\lambda^2) + (108/6125N^3)(\lambda^6 + 3\lambda^3/5 - 8/5\lambda^3) + \cdots \quad (10)$$

where N is the number of freely jointed links between entanglement points. An attempt has been made to model the orientation of PS in the blend using this equation. An example is given in *Figure 8* (curve 1) for the 90%PS blend, a composition where the network characteristics are expected to differ only slightly from those of pure PS. $\langle P_2(\cos\theta_1)\rangle$ was then calculated using equation (10) and a value of $N=29$, assuming $M_c=18\,000$ and the average number of repeat units per random link = 6, as reported for pure PS[23]. It is clear from this figure that the orientation data of PS cannot be expressed with this affine deformation model, even at small values of λ.

As pointed out by Raha and Bowden[24], the deviation from the rubber-like behaviour might be related to the breakdown of entanglements of the temporary network of the amorphous polymers, during the deformation. To account for this phenomenon, they suggested an exponential increase of the number of statistical segments between entanglement points with the draw ratio:

$$N = N_0 \exp(k\lambda) \quad (11)$$

where N_0 is the thermal equilibrium value of N for the unstrained network, and k is a temperature-dependent parameter determined by the extensibility of the chains. Taking $N_0=29$, it was not possible to fit properly the orientation data of the 90%PS blend on the basis of the Raha–Bowden model, for any value of k. Alternatively, if N_0 and k are both taken as adjustable parameters, the best fit is obtained with $N_0=2$ and $k=0.5$ (*Figure 8*, curve 2), which are unrealistic values for the PS network.

Other classic models, such as the pseudo-affine model[25] or the modified rubber-network model proposed by Nobbs and Bower[26], were tested but were unsuccessful. For example, in the pseudo-affine model, the end-to-end vector of the chains is assumed to rotate affinely during the deformation, but without extension, and $\langle P_2(\cos\theta)\rangle$ is given by an equation containing no adjustable parameter:

$$\langle P_2(\cos\theta)\rangle = 3\lambda^3/2(\lambda^3-1)\{1-(\lambda^3-1)^{-1/2}\sin^{-1}[(\lambda^3-1)/\lambda^3]^{1/2}\} - 1/2 \quad (12)$$

As can be seen in *Figure 8* (curve 3), the calculated values of $\langle P_2(\cos\theta)\rangle$ are much higher than the experimental values. The studies of Hibi *et al.*[27] and O'Neill *et al.*[28] suggest that the orientation behaviour of amorphous polymers might be described by a judicious combination of some of these models. However, we believe that such classic approaches are not appropriate since they completely ignore the relaxation motions which are crucial in such media.

Doi–Edwards theory

The molecular theory recently developed by Doi and Edwards[29–31] describes the relaxation motions, in deformed and highly entangled media, via the reptation concept introduced by de Gennes[32]. The relaxation of a suddenly deformed chain is assumed to occur in three different steps, which are well-separated in time. The first step of relaxation (step A) is a Rouse motion of a fraction of the chain between two entanglement fixed points. The second step of relaxation (step B) is a retraction of the deformed chain inside its deformed tube to recover its equilibrium curvilinear length. The last relaxation step (step C) corresponds to the reptation of the chain outside its deformed tube in order to reach an equilibrium isotropic conformation.

The Doi–Edwards topological model is extended here to the analysis of molecular orientation in PS/PVME blends. As far as the PS orientation is concerned, it is assumed that the three steps of relaxation of the Doi–Edwards theory are not significantly altered by the presence of PVME chains. The specific interactions just introduce additional entanglement points in the PS temporary network, which hinder the chain relaxation.

According to Tassin[33–35], in the case of uniaxial orientation following a step deformation, the second moment of the orientation function is given by:

$$P_2(\lambda, t) = (c/3\alpha^2)(\lambda^2 - 1/\lambda)[1+(\alpha-1)\mu_B(t)]^2\mu_A(t)\mu_C(t) \quad (13)$$

where:

$$\alpha = [\lambda + \sinh^{-1}X/(X\lambda^{1/2})]/2 \quad (14)$$

$$X = (\lambda^3 - 1)^{1/2} \quad (15)$$

λ is the draw ratio and c is a constant related to the

density of entanglements. The relaxation functions $\mu_A(t)$, $\mu_B(t)$ and $\mu_C(t)$ correspond, respectively, to steps A, B and C:

$$\mu_A(t)=1+\sum_{k=1}^{Ns}\exp(-tk^2/\tau_A) \tag{16}$$

$$\mu_B(t)=\sum_{p\,\text{odd}}(8/p^2\pi^2)\exp(-tp^2/\tau_B) \tag{17}$$

$$\mu_C(t)=\sum_{p\,\text{odd}}(8/p^2\pi^2)\exp(-tp^2/\tau_C) \tag{18}$$

where τ_A, τ_B and τ_C are, respectively, the characteristic times of relaxation of the A, B, C processes, given by:

$$\tau_A=(\xi b^2 N_s^2/6\pi^2 k_B T)^2 \tag{19}$$

$$\tau_B=2(Nc/Ne)^2\tau_A \tag{20}$$

$$\tau_C=6(Nc/Ne)^3\tau_A \tag{21}$$

where ξ is the Rouse segment friction coefficient and b is the length of the repeat unit. Nc and Ne are, respectively, the number of repeat units per chain and the number of repeat units between entanglements, N_s is the number of Rouse segments between entanglements, k_B is the Boltzmann constant and T is the temperature.

Following the same approach adopted by Tassin in the calculation of the applied stress, we have rewritten equation (13) in the form:

$$P_2(\lambda,t)=c\sum_{i=1}^{3}F_i(\lambda)\mu_i(t) \tag{22}$$

where:

$$F_1(\lambda)=(1/3\alpha^2)(\lambda^2-1/\lambda) \tag{23}$$

$$\mu_1(t)=\mu_A(t)\mu_C(t) \tag{24}$$

$$F_2(\lambda)=(2/3\alpha^2)(\alpha-1)(\lambda^2-1/\lambda) \tag{25}$$

$$\mu_2(t)=\mu_A(t)\mu_B(t)\mu_C(t) \tag{26}$$

$$F_3(\lambda)=(1/3\alpha^2)(1-1/\alpha)^2(\lambda^2-1/\lambda) \tag{27}$$

$$\mu_3(t)=\mu_A(t)\mu_B^2(t)\mu_C(t) \tag{28}$$

For a continuous mode of stretching, and assuming the validity of the Boltzmann superposition principle[36], the second moment of the orientation function is given by:

$$P_2(\lambda,t)=-c\sum_{i=1}^{3}\int_{-\infty}^{t}\mu_i(t-t')\frac{\mathrm{d}}{\mathrm{d}t'}[F_i(\lambda,\lambda')]\,\mathrm{d}t' \tag{29}$$

$$F_i(\lambda,\lambda')=F_i(\lambda(t)/\lambda'(t)) \tag{30}$$

In our experiments, the sample was stretched to a given draw ratio λ, with a constant linear strain rate $\dot{\varepsilon}=\mathrm{d}\lambda/\mathrm{d}t$. The limiting conditions are:

$$\begin{array}{ll}\text{For } t\leqslant 0,\ \lambda=1 & \\ \text{For } t>0,\ \lambda=1+\dot{\varepsilon}t & \rightarrow\ (\lambda,\lambda')=(1+\dot{\varepsilon}t)/(1+\dot{\varepsilon}t')\end{array}$$

Taking into account these conditions, equation (29) is modified as follows:

$$P_2(\lambda,t)=c\sum_{i=1}^{3}\left\{F_i(\lambda)\mu_i(t)+\int_0^t F_i[(1+\dot{\varepsilon}t)/(1+\dot{\varepsilon}t')]\frac{\partial}{\partial t'}[\![\mu_i(t-t')]\!]\,\mathrm{d}t'\right\} \tag{31}$$

or

$$P_2(\lambda)=c\sum_{i=1}^{3}\left\{F_i(\lambda)\mu_i[(\lambda-1)/\dot{\varepsilon}]+\int_1^{\lambda}F_i(\lambda/\lambda')\frac{\partial}{\partial\lambda'}[\![\mu_i((\lambda-\lambda')/\dot{\varepsilon})]\!]\,\mathrm{d}\lambda'\right\} \tag{32}$$

It is observed that, for a given λ, $P_2(\lambda)$ depends upon parameters c, τ_A, τ_B and τ_C, since $\dot{\varepsilon}$ is known from the experimental conditions.

It is difficult to model the orientation data using the general form of equation (32), since for a given value of c, it is always possible to adjust independently the parameters τ_A, τ_B and τ_C to fit the experimental data. In other words, the set (c, τ_A, τ_B, τ_C) is not unique, for a given composition. However, it can be noticed that equation (32) is sensitive to the different relaxation times τ_i only if $\dot{\varepsilon}\tau_i$ lies between 0.25 and 25; this has been tested numerically, since the relative variation of $\langle P_2(\cos\theta)\rangle$ outside these limits is well below 10%, which is the limit of sensitivity of the experimental measurements. These limiting values correspond to τ_i between 10^2 and 10^4 s, since the effective strain rate used here is $\dot{\varepsilon}=0.0025\ \mathrm{s}^{-1}$. In other words, when τ_i is out of this range, the relaxation process is either too fast or too slow, as compared to the experimental time-scale, to be detected in the orientation measurements. Taking this into account, the following procedure has been adopted in order to reduce the number of adjustable parameters.

First, it must be realized that, by taking T_c as a reference temperature, the samples are stretched at different distances from T_g. For example, $T-T_g$ is 4 K for the 90%PS blend while it is 53 K for the 50%PS blend. Hence, the relaxation times are expected to vary by several orders of magnitude as a function of composition. Second, the relaxation time of the PS chains in the blend can be taken to be of the same order of magnitude as that of pure PS, at the same reference temperature $T-T_g$. Some typical values of the PS relaxation time, which have been determined by different techniques[37–40], are summarized in *Table 1*. We have recalculated each of these values for a reference temperature $T_0=392$ K and $M_w=300\,000$. The range of values thus obtained is also given in *Table 1*. The temperature correction has been made using the Williams–Landel–Ferry (WLF) equation[41]:

$$\log(\tau_T/\tau_0)=-A(T-T_0)/(B+T-T_0) \tag{33}$$

where $A=9.2$ and $B=68.8$ K are the WLF coefficients derived from the data of Plazek[42]. The molecular weight correction, as well as the evaluation of other relaxation times from experimental data, have been made using equations (20) and (21). *Table 1* indicates wide scatter in the data; in our opinion, this is mainly due to the difference in the techniques used. However, it is clear that, at 392 K for example, the relaxation processes A and C in pure PS are outside the range of sensitivity of the experimental orientation measurements. In order to check this point, and also to properly select reference values of the relaxation times, orientation measurements have been made on pure PS at 392 K, which corresponds to T_g+10. As can be seen from *Figure 9*, the experimental data are properly fitted using only two parameters, c and τ_B, assuming that $\mu_A(t)$ and $\mu_C(t)$ are ≈ 1. The

Table 1 Relaxation times τ_A, τ_B and τ_C of pure polystyrene taken from the literature. In the last row, values are calculated for $T_0 = 392$ K and a molecular weight of 300 000, as indicated in the text

T (K)	M_w $\times 10^3$	τ_A (s)	τ_B (s)	τ_C (s)	Ref.
390	700	1–13	3×10^3–4×10^4 [a]	3.5×10^5–4.7×10^6	35
433	35–2700	0.9–5.4	2.5×10^{-3}–89	1.5×10^{-2}–4×10^4 [a]	36
200	200	5.5	25[a]	833	37
393	100–900	5.6[a]	3.5×10^2–2.8×10^4	5.7×10^3–4.2×10^6	38
392	300	0.5–7	2.9×10^2–3.9×10^3	1.5–19×10^4	

[a] Experimental values

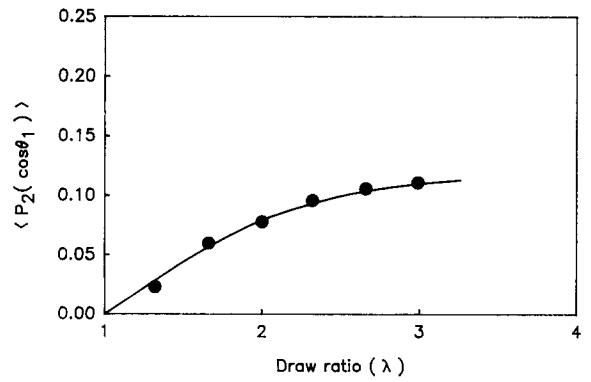

Figure 9 Orientation function $\langle P_2(\cos\theta)\rangle$ of pure PS as a function of the draw ratio, λ, at 392 K and a stretching rate of 5 cm min^{-1}. The continuous line is drawn using equation (32) with $c = 0.09$, $\tau_B = 300$ s, $\dot{\varepsilon} = 0.0025$ s^{-1}

relaxation time derived from this fit is $\tau_B = 300$ s, which leads to $\tau_A = 0.54$ s (equation (20)) and $\tau_C = 1.5 \times 10^4$ s (equations (20, 21)). These values are in agreement with the literature data (*Table 1*).

Starting from these reference values, the characteristic relaxation times of pure PS have been calculated, at different temperatures $T - T_g$ corresponding to those of the different blends (*Table 2*). It can be noticed that the A process is expected to be fast compared to the experimental time-scale, in the whole temperature range investigated. Furthermore, at $T - T_g < 20$ K, the C process is expected to be too slow, while at $T - T_g > 20$ K, the B process is too fast. It is then possible to fit the experimental data, at each blend composition, using only one relaxation time as an adjustable parameter (*Figure 5*), namely, τ_B at $T - T_g \leqslant 20$ K (i.e. 90, 80 and 70% PS blends) and τ_C at $T - T_g > 20$ K (i.e. 60 and 50%PS blends). It should be noted that the shape of the curves is influenced mainly by the relaxation time parameter, whereas the parameter c, which is a multiplicative constant in equation (32), affects only the magnitude of $\langle P_2(\cos\theta)\rangle$[19]. In addition, the decrease of $\langle P_2(\cos\theta)\rangle$ at high values of λ is observed experimentally for the 60% and 50%PS blends and is theoretically confirmed. This is due to the fact that, at high λ, the time of stretching becomes larger than the relaxation time τ_C, which leads to the progressive decrease in orientation.

The analysis of the results on the basis of the Doi–Edwards theory allows us to understand the orientation behaviour of the PS/PVME blend, at $T_C - 62$. By keeping the distance to T_C constant, as in this study, the difference between the stretching temperature and T_g increases progressively with PVME content in the blend.

Table 2 Relaxation times of pure polystyrene calculated at different reference temperatures, $T - T_g$, using equation (33)

$T - T_g$ (K)	τ_A (s)	τ_B (s)	τ_C (s)
4	4	2270	1.2×10^5
10	0.54	300	1.5×10^4
20	3.6×10^{-2}	20	1.0×10^3
39	1.0×10^{-3}	5.6×10^{-1}	28
53	1.6×10^{-4}	8.7×10^{-2}	4.3

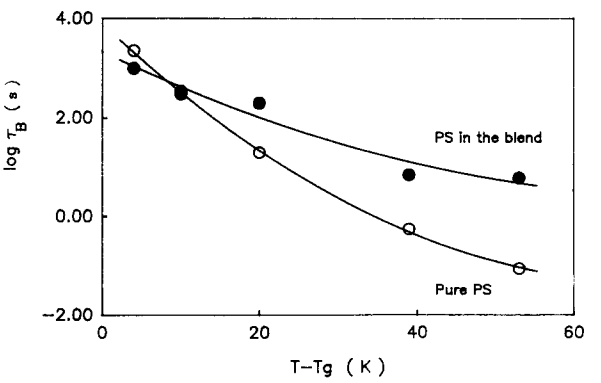

Figure 10 Relaxation time τ_B of pure PS and of PS in PS/PVME blends, as a function of the distance from T_g

Therefore, the free volume of the chains increases, leading to faster relaxation and lower degree of orientation. For instance, when w_2 decreases from 0.9 to 0.5, the free volume fraction of the blend, calculated assuming a simple rule of additivity, increases from 0.025 to 0.036, and the PS relaxation time decreases correspondingly by two orders of magnitude (*Figure 10*). In that context, the more rapid decrease of PVME orientation as compared to PS orientation, illustrated in *Figure 6*, can be explained by a more rapid relaxation of PVME as compared to PS. This may be attributed to its lower molecular weight, as expected from the theory. On the other hand, it can be noticed from *Figure 10* that, for a given reference temperature $T - T_g$, the relaxation time of PS chains in the blend is, in general, higher than that in pure PS. Moreover, the difference between the relaxation time in pure PS and in the blend increases with the amount of PVME. This behaviour reflects the influence on orientation of specific interactions between PS and PVME, which modify the local environment of the PS chains and hinder their relaxation. Since the probability

of heteromolecular contacts increases with w_2, this influence is expected to become stronger as PVME is introduced in the blend. The effect of specific interactions on molecular orientation of PS/PVME blends will be analysed in more detail in a forthcoming paper[43].

From another point of view, it is worth noting that the overall orientation of the blend can also be modelled by the constitutive equation (32) assuming that the two dissimilar chains behave like a hypothetical 'equivalent chain', due to the presence of specific interactions between them (*Figure 2*). However, the parameters derived from such an analysis characterize the overall behaviour of the two polymers and cannot be attributed specifically to one of them.

CONCLUSION

The linear relation between the overall orientation and Young's modulus, observed at the initial stage of deformation of PS/PVME blends, is satisfactorily explained by the rubber elasticity theory. However, the classical models of deformation derived from this theory fail to describe the strain–orientation relation at larger deformations, mainly because the relaxation contribution, which plays a crucial role in amorphous blends, must be considered at larger deformations. On the other hand, the relation between strain and orientation has been successfully modelled by a constitutive equation derived from the Doi–Edwards theory, which integrates explicitly the chain relaxation motions. The relaxation time of PS chains in the blend, derived from this analysis, was found to be higher than that in pure PS, for the same reference temperature $T-T_g$. This behaviour emphasizes the importance of specific interactions and their influence on the dynamics of the chains in a blend.

It must be pointed out that this theoretical approach gives useful information about the orientation process in the PS/PVME blend, even though the Doi–Edwards model was developed originally for simple amorphous systems. However, a more rigorous approach, using the concept of the tube model and integrating explicitly the specific interaction contribution in the form of an external potential, has to be developed. Such an approach has been proposed to predict the linear viscoelastic behaviour of compatible polymer mixtures[44,45], but this model is valid only in the linear viscoelastic region and cannot be directly transposed for large deformations.

ACKNOWLEDGEMENTS

This study was supported by grants from the Natural Sciences and Engineering Research Council of Canada and the Department of Education of the Province of Québec (FCAR and Actions Structurantes programmes).

REFERENCES

1 Hubbell, D. S. and Cooper, S. L. *J. Appl. Polym. Sci.* 1977, **21**, 3035
2 Hubbell, D. S. and Cooper, S. L. *Adv. Chem. Ser.* 1979, **176**, 517
3 Lefèbvre, D., Jasse, B. and Monnerie, L. *Polymer* 1984, **25**, 318
4 Bouton, C., Arrondel, V., Rey, V., Sergot, Ph., Manguin, J. L., Jasse, B. and Monnerie, L. *Polymer* 1989, **30**, 1414
5 Zhao, Y., Jasse, B. and Monnerie, L. *Polymer* 1989, **30**, 1643
6 Parmer, J. F., Dickinson, L. C., Chien, J. C. W. and Porter, R. S. *Macromolecules* 1987, **20**, 2308
7 Chu, C. W., Dickinson, L. C. and Chien, J. C. W. *J. Appl. Polym. Sci.* 1990, **41**, 2311
8 Oultache, A. PhD Thesis, Université Pierre et Marie Curie, Paris, 1992
9 Han, C. C., Okada, M., Muroga, Y., McCrackin, F. L., Bauer, B. J. and Tran-Cong, Q. *Polym. Eng. Sci.* 1986, **26**, 3
10 Han, C. C., Sauer, B. J., Clark, J. C., Muroga, Y., Matsushita, Y., Okada, M., Tran-Cong, P., Chan, T. and Sanchez, I. C. *Polymer* 1988, **29**, 2004
11 Ward, I. M. 'Structure and Properties of Oriented Polymers', Applied Science Publishers, London, 1975
12 Bower, D. I. *J. Polym. Sci., Phys. Edn* 1981, **19**, 93
13 Samuels, R. J. 'Structured Polymer Properties', Wiley, London, 1974
14 Stein, R. S. in 'Polymer Blends' (Ed. D. R. Paul), Academic Press, London, 1978
15 Lefèbvre, D., Jasse, B. and Monnerie, L. *Polymer* 1982, **23**, 706
16 Hashimoto, T., Masahiko, M. and Hasegawa, H. *J. Chem. Phys.* 1986, **85**, 10
17 Lefèbvre, D., Jasse, B. and Monnerie, L. *Polymer* 1981, **22**, 1616
18 Faivre, J. P., Jasse, B. and Monnerie, L. *Polymer* 1985, **26**, 879
19 Abtal, E. PhD Thesis, Université Laval, 1990
20 Treloar, L. R. G. 'The Physics of Rubber Elasticity' 2nd Edn, Oxford University Press, London, 1958, Ch. X
21 Read, B. E. *Polymer* 1962, **3**, 143
22 Roe, R. J. and Krigbaum, W. R. *J. Appl. Phys.* 1964, **35**, 2215
23 Aharoni, S. M. *Macromolecules* 1983, **16**, 1722
24 Raha, S. and Bowden, P. B. *Polymer* 1972, **13**, 174
25 Ward, I. M. *Proc. Phys. Soc.* 1962, **80**, 1176
26 Nobbs, J. H. and Bower, D. I. *Polymer* 1978, **19**, 1100
27 Hibi, S., Maeda, M., Kubota, H. and Miura, T. *Polymer* 1977, **18**, 137
28 O'Neill, M. A., Duckett, R. A. and Ward, I. M. *Polymer* 1988, **29**, 54
29 Doi, M. and Edwards, S. F. *J. Chem. Soc. Faraday Trans. 2* 1978, **74**, 1789
30 Doi, M. *J. Polym. Sci., Polym. Chem. Edn* 1980, **18**, 1005
31 Doi, M. and Edwards, S. F. 'The Theory of Polymer Dynamics', Clarendon, Oxford, 1986
32 de Gennes, P. G. 'Scaling Concepts in Polymer Physics', Cornell University Press, Ithaca, 1979
33 Tassin, J. F. PhD Thesis, Université Pierre et Marie Curie, Paris, 1986
34 Thirion, P. and Tassin, J. F. *J. Polym. Sci., Polym. Phys. Edn* 1983, **21**, 2097
35 Tassin, J. F. and Monnerie, L. *Macromolecules* 1988, **21**, 1846
36 Chang, W. V. and Bloch, R. *J. Polym. Sci., Polym. Phys. Edn* 1977, **15**, 923
37 Boué, F., Nierlich, M., Jannink, G. and Ball, R. *J. Phys.* 1982, **43**, 137
38 Montfort, J. P., Marin, G. and Monge, P. *Macromolecules* 1984, **17**, 1551
39 Tassin, J. F., Thirion, P. and Monnerie, L. *J. Polym. Sci., Polym. Phys. Edn* 1983, **21**, 2109
40 Tassin, J. F., Monnerie, L. and Fetters, L. J. *Macromolecules* 1988, **21**, 2404
41 Ferry, J. D. 'Viscoelastic Properties of Polymers', Wiley, New York, 1980
42 Plazek, D. J. *J. Phys. Chem.* 1965, **69**, 3480
43 Abtal, E. and Prud'homme, R. E. in preparation
44 Han, C. D. and Kim, J. K. *Macromolecules* 1989, **22**, 1914
45 Han, C. D. and Kim, J. K. *Macromolecules* 1989, **22**, 4292